RSC Advances

ROYAL SOCIETY OF CHEMISTRY

www.rsc.org/advances

Journal Name

RSCPublishing

ARTICLE

Thiol-ene Adhesives from Clove Oil Derivatives

Brian R. Donovan,[a] Jared S. Cobb,[a] Ethan F. T. Hoff,[a] and Derek L. Patton[a*]

Cite this: DOI: 10.1039/x0xx00000x

Received ooth January 2012,
Accepted ooth January 2012

DOI: 10.1039/x0xx00000x

www.rsc.org/

This paper reports the synthesis of catechol-functionalized thiol-ene polymer networks as photocurable adhesives, where the adhesive interactions are derived from 4-allylpyrocatechol – a monofunctional alkene readily obtained from natural products of Syzygium aromaticum flower buds (clove). The thiol-ene photopolymerization process enables rapid cure times, low energy input, and solvent-free processing. The resulting polymer networks show improved macroscopic adhesion to a variety of substrates – including glass, marble, aluminum, and steel – by varying the concentration of 4-allylpyrocatechol in the network. Additionally, the effects of the catechol moiety on polymerization kinetics, thermomechanical, and mechanical properties were determined by comparing the synthesized catechol moiety to a series of control monomers such as eugenol (one phenol group) and methyl eugenol (no phenol groups).

Introduction

The use of commercial adhesives is ever-growing due to their cost effectiveness, high design flexibility, and ability to join dissimilar materials.[1] Because of these features, adhesives have found use everywhere from the household to aerospace applications. Simultaneously, the global culture, both industrially and academically, is beginning to make a conscious effort to further the use of environmentally friendly and sustainable processes and products. Naturally, the adhesive industry has followed suit and research in bio-inspired adhesives has moved rapidly forward in the past decade. Several examples of robust adhesive systems exist in nature, including that of the marine mussel, which is characterized by its unique ability to bond under wet, harsh, intertidal conditions to complex heterogeneous substrates. While this naturally occurring adhesive system contains a complex variety of proteins,[2] the mussel plaque proteins can contain near 30 mol % of the amino acid 3,4-dihydroxyphenylalanine (DOPA), responsible, in part, for both the cohesive and adhesive interactions of the mussel's adhesive plaques.[3, 4] The catechol moiety present in DOPA is capable of adhesive interactions via hydrogen bonding,[5, 6] π-π aromatic interactions, and metal-ligand complexations,[4, 5, 7, 8] and also cohesive interactions via di-DOPA linkages[9] by oxidative,[10, 11] enzymatic,[10-12] or redox-induced radical chemistry.[5, 9, 13] The proteins located in the interfacial plaque of the mussel's adhesive byssus structure can be harvested however, this process is time consuming, expensive, and yields minimal material. Alternatively, DOPA-analogues can be synthesized in a variety of ways to develop biomimetic adhesives, including from naturally occurring small molecules.[14, 15]

The earliest work published on synthetic, DOPA-containing polymers focused on designing synthetic polypeptides,[16-18] and has since expanded to include linear, [19-23] and crosslinked polymeric systems.[22, 24, 25] While polypeptide synthesis, thermal radical polymerization, and oxidative crosslinking have been successfully utilized to develop both bio- and synthetic adhesives,[19, 22] photopolymerization offers several advantages over conventional radical polymerizations, particularly in the case of elastomers and thermosets. These advantages include rapid, large area cures, ambient conditions, low energy requirements, and solvent free compositions. In general, visible or UV photopolymerization facilitates eco-friendly polymerization processes on a potentially industrial scale. Recent literature contains several examples of photopolymerized, DOPA-analogue containing networks. Chung et al.[24] photopolymerized dopamine methacrylamide and 2-methoxyethyl acrylate copolymers while varying the amount of crosslinker to investigate the effect changes in viscoelastic properties had on wet and dry adhesion. Lightly crosslinked networks showed the highest work of adhesion under wet conditions, while the non-crosslinked system showed the highest work of adhesion under dry conditions. More recently, Xue et al. photopolymerized a monofunctional[25] and multifunctional[26] catechol containing methacrylate monomer, crosslinked with modified poly(vinyl alcohol) – a system showing adhesion strength increases upwards of 150% compared to control samples. Acrylate and methacrylate polymer networks have found common use in a wide range of applications, but in general, yield heterogeneous networks and suffer from oxygen inhibition, resulting in longer cure times.[27]

UV thiol-ene photopolymerizations eliminate some of the drawbacks associated with acrylate or methacrylate polymerizations, including oxygen inhibition and heterogeneous network structure,[28-30] due to the unique thiol-ene polymerization mechanism. Thiol-ene networks form via a free-radical step-growth process facilitated by rapid chain transfer, which generates highly homogenous networks resulting in well-defined physical and mechanical properties, typically reflected by a narrow glass transition (T_g). The well-defined properties of thiol-enes have led to their utilization in a wide range of functional materials[28, 30, 31] including recent work by our group[32] in which dopamine acrylamide (DAm) was incorporated into a thiol-ene network to generate adhesive functionality, and also to investigate how the catechol moiety influenced network properties. Their findings showed that DAm imparted adhesive functionality to the thiol-ene system, while influencing network properties by changes in crosslink density and the amount of internetwork hydrogen bonding. While the work by Sparks et al.[32] was the first to incorporate a DOPA analogue into a thiol-ene network, DAm was not soluble without the use of small amounts of DMF, thus diminishing the eco-friendly aspects of solvent-free photopolymerizations.

In this work, we aim to develop a ternary thiol-ene network, based on a catechol monomer (4-allylpyrocatechol, EugOH) incorporated with pentaerythritol triallyl ether (APE), and pentaerythritol tetra(3-mercaptopropionate) (PETMP). 4-allylpyrocatechol is readily obtained from precursors such as eugenol or methyl eugenol – two natural products predominately extracted from the essential oils of *Syzygium aromaticum* flower buds (commonly known as clove buds) by hydrodistillation.[33, 34] The energy efficiency and solvent-free conditions of photopolymerization, along with adhesive moieties readily available from natural product derivatives, enable the development of an eco-friendly route to thiol-ene adhesives. The robustness of thiol-ene photopolymerizations of APE-PETMP networks makes it an ideal system for studying the influence the catechol moiety has on photopolymerization kinetics, thermomechanical, mechanical, and adhesive properties. To further elucidate the influence of the catechol moiety, analogous APE-PETMP networks will be synthesized containing the monofunctional monomers methyl eugenol (MeEug) and eugenol (Eug).

Experimental

Materials

All reagents and solvents were obtained at the highest purity available from Aldrich Chemical Co. and used without further purification unless otherwise specified. Methyl eugenol and eugenol were purchased as natural grade from Aldrich. Pentaerythritol triallyl ether, and sodium sulfate were obtained from Sigma-Aldrich; Irgacure 2022 was obtained from BASF; and pentaerythritol tetra(3-mercaptopropionate) was obtained from Bruno Bock.

Synthesis of triethylsilane-eugenol (EugTES)

EugTES was synthesized using a modified method developed by Hawker et. al.[14] In a typical reaction, 8.00 g (45 mmol) of methyl eugenol was dissolved into 50 mL of dry toluene and a catalytic amount (0.25 wt%) of tris(pentafluorophenyl)borane (TPFPB), under an N_2 atmosphere, followed by the slow addition of 16 mL (100 mmol, 2.2 mol equiv.) triethylsilane. Methane gas was rapidly evolved as the reaction proceeded. After reaction completion was determined by ^{1}H NMR, the catalyst was removed by passing the reaction mixture through a neutral alumina plug with CH_2Cl_2 as the eluent, followed by removal of solvent under vacuum to recover the pure product as a colorless oil (Yield, 93%); δ_H (300MHz, $CDCl_3$; Me_4Si) 0.70-0.78 (12H, m, CH_2), 0.96-1.01 (18H, t, CH_3), 3.25 (2H, d, CH_2), 5.00-5.05 (2H, m, $CH=CH_2$), 5.87-6.00 (1H, m, $CH=CH_2$), 6.58-6.74 (3H, m, Ar-H); δ_C (300MHz, $CDCl_3$, Me_4Si) 5.06, 6.68, 39.4, 115.3, 120.2, 120.9, 121.3, 133.0, 137.8, 144.9, 146.5.

Synthesis of 4-allylpyrocatechol (EugOH)

8.00 g EugTES (21 mmol) was dissolved in 10 mL of THF and purged with N_2 for 45 minutes. The solution was then transferred, under N_2, to a reaction vessel containing HCl solution, and mixed rapidly. The reaction proceeded quickly and completion was confirmed via thin layer chromatography. The organic layer was extracted into CH_2Cl_2 and then washed with H_2O, followed by drying and filtration. The solvent was removed via vacuum to recover the pure product as a white solid (Yield, 54%); δ_H (300MHz, $CDCl_3$; Me_4Si) 3.25 (2H, d, CH_2), 5.03-5.08 (2H, m, $CH=CH_2$), 5.24 (1H, s, OH), 5.32 (1H, s, OH), 5.86-5.99 (1H, m, $CH=CH_2$), 6.62-6.81 (3H, m, Ar-H); δ_C (300MHz, $CDCl_3$, Me_4Si) 39.5, 115.4, 115.6, 121.1, 133.4, 137.6, 141.5, 143.3.

Film Preparation

Aluminium Q-panels (A-36 with a smooth mill finish), steel Q-panels (QD-36 with a smooth finish), and white polished venation marble, obtained from Lowe's Home Improvement, were prepared by wiping away any oils or dust in a downward direction. Glass substrates were cleaned using acetone and ethanol. Monomer resins, prepared as previously described were drawn down across various substrates at a thickness of 2 mils (~ 50 μm). The samples were subsequently cured for 20 minutes under a medium pressure mercury UV lamp at an intensity of 15 mW/cm^2.

Characterization

A Varian Mercury Plus 300 MHz NMR spectrometer operating at a frequency of 300.13 MHz with VNMR 6.1C software was used for structure analysis of EugTES and EugOH. Kinetic data was obtained using real time FTIR (RT-FTIR) spectroscopy by determining the conversions of the thiol and alkene group functionalities. The RT-FTIR studies were conducted using a Nicolet 8700 spectrometer with a KBr beam splitter and a MCT/A detector with a 320−500 nm filtered ultraviolet light source. Each sample was sandwiched between two NaCl plates

and exposed to a UV light with an intensity of approximately 20

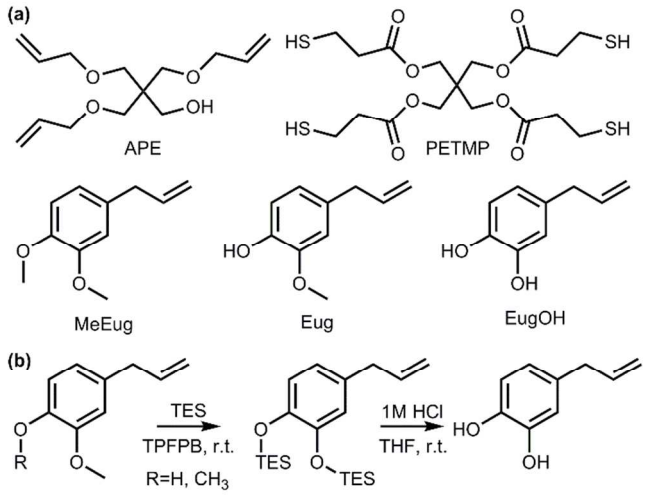

Fig. 1 (a) Chemical structures of thiol-ene monomers, including the various clove oil derivatives. (b) Synthetic scheme for the preparation of 4-allylpyrocatechol (EugOH) from methyl eugenol. Acronyms: TES (triethylsilane), TPFPB (tris(pentafluorophenyl)borane).

mW/cm^2. A series of scans were recorded, where spectra were taken approximately 3 scan/s with a resolution of 4 cm^{-1}. Dynamic mechanical analysis (DMA) was performed using a TA Instruments Q800 dynamic mechanical analyzer in tension film mode equipped with a gas cooling accessory. Samples were secured and the strain applied was 0.05%. Samples were heated from −40 to 60 °C at a ramp rate of 2 °C/min. Mechanical testing was performed using a MTS Insight material testing machine equipped with a 10 kN load cell and pre-set to collect 10 data points per second. Dog bone samples with cross-sectional dimensions of 0.120 in ± 0.08 in and 0.59 in ± 0.05 in (thickness and width) were carefully centered in clamps and deformed in tensile mode at a strain rate of 0.2 in/min. Young's modulus was determined from the initial linear elastic region of the stress−strain curve. Strain at break was determined concurrently during the tensile tests.

Adhesion Testing

Cross-hatch adhesion was measured using a Cross-Cut Tape Test Kit by Precision Gauge and Tool Company according to ASTM D-3359.[35] The adhesive properties of the materials from the cross-hatch test are graded on a scale of 5B to 0B based on approximate percentage of film removed by the tape. A sample classified as 5B can be described as a lattice where the edges of the cut films remain completely smooth and intact. Classes 4B-1B describe the degree in which the film has been removed from the lattice, where less than 5% of the film is removed in 4B and a sample described as 1B has 35 – 65% of the film removed from the lattice. If greater than 65% of the film has flaked or delaminated from the substrate, it is classified as 0B. Bulk adhesion was measured via a single-lap-joint adhesively bonded glass sample according to a modified version of ASTM D-1002.[36] Thiol-ene formulation was applied to glass substrates which were then overlapped (1.0 x 25.0 cm) with uniform surface coverage, followed by a 20 minute cure under UV light at an intensity of 15 mW/cm^2. All trials were performed using an MTS Insight material testing machine equipped with a 10 kN load cell, moving with a crosshead speed of 0.5 cm/ min. At least five trials were performed per sample to obtain a statistical average.

Results and discussion

Synthesis of EugOH

The eugenol and triethylsilane protection/deprotection sequence developed by Hawker et al.[14], shown in Figure 1, provides a facile and mild synthetic procedure to yield an unsaturated catechol monomer. Triethylsilane, in the presence of TPFPB, is susceptible to nucleophilic attack from both hydroxy and methoxy functional groups, generating the silyl ether upon release of hydrogen and methane gas.[37] Triethylsilane can then be easily removed under mild acidic conditions to generate the catechol moiety. The synthesized 4-allylpyrocatechol (for NMR spectra, see Fig. S3 and Fig. S4), showed improved solubility over acrylamide containing catechol monomers,[24, 32] and was successfully incorporated into thiol-ene resins without the use of additional solvent or heat, maintaining the green aspects of thiol-ene photopolymerization.

Photopolymerization and Kinetics of Ternary Thiol-Ene/EugOH Polymer Networks

Thiol-ene polymer networks, based on a trifunctional alkene and a tetrafunctional thiol, were synthesized containing various mol % of monofunctional alkenes, including methyl eugenol, eugenol, and 4-allylpyrocatechol (Figure 1). All monofunctional alkenes were fully soluble in network precursors. The solubility of the eugenol derivatives in the thiol-ene resin precursors is a major distinction from our previous work with dopamine acrylamide,[32] which was crystalline, insoluble, and required DMF for homogeneous photopolymerization. Catechol and phenol functionalities are powerful radical scavengers making it a common practice to carry out radical-mediated polymerizations using protected versions of catechol monomers.[38] However, recent work by our group and others[25, 26, 32] has demonstrated that it is possible to generate polymer structures in photopolymerizations of our eugenol derivative series. The IR spectra for formulations containing EugOH, pre-polymerization, are shown in Figure 2, with highlighted thiol and alkene peaks at 2570 cm^{-1} (green box) and 3078 cm^{-1} (blue box), respectively (see Figs. S5-S8 for MeEug and Eug FTIR spectra). Figure 3 shows the resulting IR spectra, post UV exposure, of the EugOH formulations and the corresponding disappearance of both the thiol and alkene peak. Photopolymerization kinetics were monitored in real time, by measuring the change in area of the thiol and alkene peaks upon UV exposure. The change in area was converted to percent conversion values and plotted against time for formulations containing each of the eugenol

derivatives. Final conversion values extracted from the conversion plots are presented in Table 1. The thiol-ene

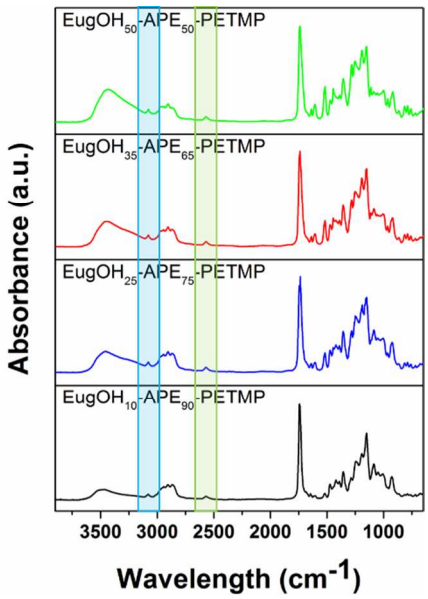

Fig. 2 *FTIR of unpolymerized EugOH-APE-PETMP monomer resins.*

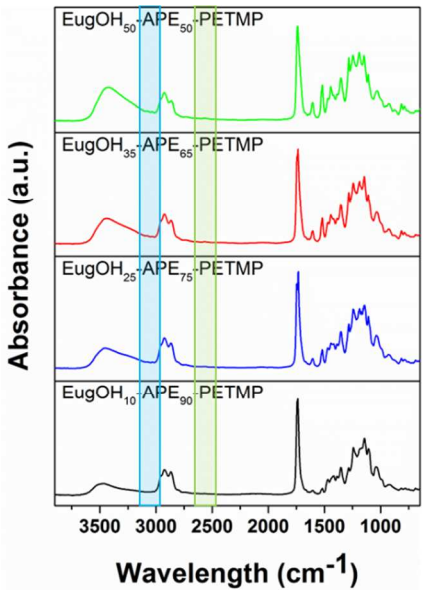

Fig. 3 FTIR of polymerized EugOH-APE-PETMP ternary polymer networks.

photopolymerization of networks containing MeEug showed quantitative thiol and alkene conversion at all mol % loadings (Figure S9). Eug exhibited incomplete conversions only in formulations containing 35 mol % and 50 mol %, with conversion values reaching 95% and 94%, respectively (Figure S10). The catechol containing EugOH however, showed more significant decreases in conversion with final values decreasing from 89% at 25 mol % loading, down to 80% at 50 mol % loading as shown in Figure 4. Figure 4 additionally shows evidence of retardation, observed as a decrease in the slope of the initial portion of the RTIR conversion plots. A decrease in initial polymerization rate with increasing EugOH concentrations was observed and can be attributed to the retarding effects of the catechol (similar trends are seen in the

Table 1 Conversion percentage values of ternary-APE-PETMP networks containing methyl eugenol, eugenol, and 4-allypyrocatechol.

Monofunctional	Alkene ratio				
Monomer	0:100	10:90	25:75	35:65	50:50
MeEug	>99	>99	>99	98	98
Eug	>99	>99	96	95	94
EugOH	>99	>97	89	86	80

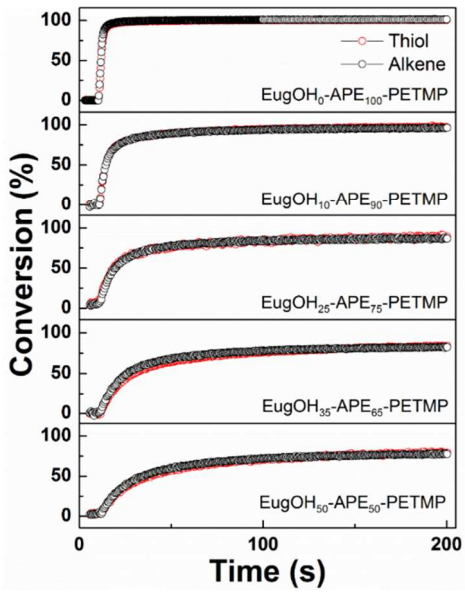

Fig. 4 *Kinetic plots of conversion vs. time for EugOH-APE-PETMP thiol-ene networks. (a) 0 mol % EugOH, (b) 10 mol % EugOH, (c) 25 mol % EugOH, (d) 35 mol % EugOH, (e) 50 mol % EugOH.*

Eug system, containing a phenol moiety, but not in the MeEug system, which has no retarding group). The kinetic results are consistent with previous work done in our group using dopamine acrylamide containing thiol-ene networks,[32] as well as recent work by Ai et. al[39] which showed final conversion values and initial rate values decrease as the concentration of a catechol-containing monomer was increased within an acrylate system polymerized by radical-mediated photopolymeization. While retardation becomes more significant at higher concentrations of EugOH, ternary thiol-ene networks were still effectively formed via UV photopolymerization.

Thermomechanical and Mechanical Properties

The thermomechanical properties of the catechol-derivative thiol-ene polymer networks were investigated using DMA, where the glass transition temperature (T_g) was determined in strain film mode at a heating rate of 2 °C/min from the peak maximum of the tan δ curve. T_g values and additional thermomechanical properties of the various ternary thiol-ene networks are presented in Table 2. Figure 5 shows the change of the storage modulus for the EugOH-APE-PETMP networks as a function of temperature. A clear decrease in the rubbery

storage modulus was observed with increasing EugOH concentrations due to a decrease in crosslink density upon greater incorporation of the monofunctional monomer in the network. The same trend

Table 2. Thermomechanical and mechanical properties of ternary APRE-PETMP networks containing methyl eugenol, eugenol, and 4-allylpyrocatechol.

Alkene Ratio	T_g (°C)	fwhm (°C)[a]	E'Rub, T_g+40 °C (MPa)	ρ_x (10^{-3}mol cm^{-3})[b]	Young's Modulus (MPa)	Strain at Break (%)
MeEug-APE-PETMP						
0:100	9.3	11.9	29.8	3.71	13.7	25.6
10:90	4.7	13.0	18.4	2.33	10.4	28.1
25:75	3.4	12.6	14.6	1.85	5.82	28.7
35:65	2.4	13.5	8.34	1.06	3.60	28.7
50:50	-0.67	13.7	1.90	0.244	1.26	42.3
Eug-APE-PETMP						
0:100	9.3	11.9	29.8	3.71	13.7	25.6
10:90	1.2	13.1	18.3	2.33	9.28	29.8
25:75	-0.67	15.9	9.76	1.25	5.13	29.5
35:65	-0.98	13.3	4.56	0.586	2.97	26.4
50:50	-1.4	13.8	1.46	0.188	0.861	69.9
EugOH-APE-PETMP						
0:100	9.3	11.9	29.8	13.7	13.7	25.6
10:90	-0.71	11.2	15.5	7.36	7.36	36.7
25:75	-3.0	12.3	4.70	3.55	3.55	39.7
35:65	-3.8	13.7	3.03	1.90	1.90	51.1
50:50	-7.2	19.9	0.249	0.266	0.266	135

[a]fwhm obtained from the tan δ curves. [b]Crosslink density (ρ_x).

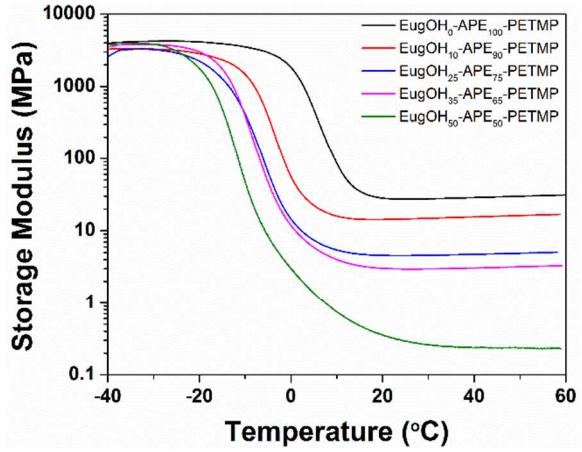

Fig. 5. Storage modulus vs. temperature for the EugOH-APE-PETMP polymer networks with varying concentrations of EugOH (0-50 mol %).

in rubbery storage modulus was observed in MeEug (Figure S11) and Eug (Figure S13) networks. In order to develop a quantitative description of the observed trends in the rubbery storage modulus, the crosslink density (ρx) of the polymer networks was estimated from the rubbery plateau storage modulus at Tg + 40 °C according to the theory of rubber elasticity,[40] $\rho_x = E'/2(1+\gamma)RT$, where E' is the rubbery storage modulus at temperature T, R is the gas constant, and γ is Poisson's ratio, which is assumed to be 0.5 for incompressible networks. Crosslink density values decrease with increasing monofunctional monomer content (Table 2) and also decrease from MeEug to Eug to EugOH at the equivalent loading percentages. The decreasing conversion with increasing hydroxyl content, and therefore increasing radical scavenging ability, likely contributes to the trends observed in the rubbery plateau regime.

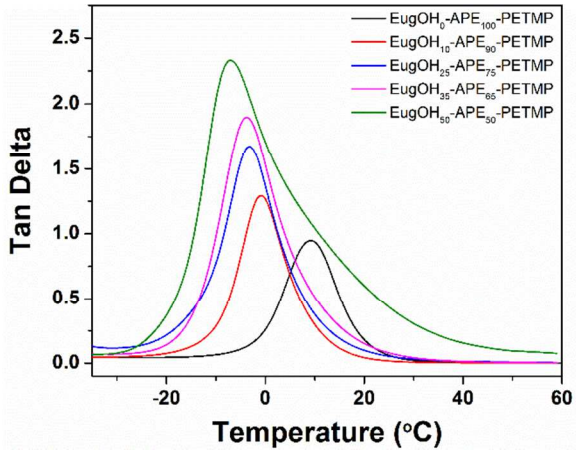

Fig. 6 Tan δ vs. temperature for the EugOH-APE-PETMP polymer networks with varying concentrations of EugOH (0-50 mol %).

Figure 6 shows the tan δ curves for the ternary EugOH-APE-PETMP networks with increasing EugOH concentration. The neat system shows a narrow glass transition temperature at 9.3 °C, which is typical of the APE-PETMP thiol-ene system with comparable loadings of photoinitiator.[41] As the concentration of EugOH is increased, the Tg systematically decreases to -7.2 °C for 50 mol % EugOH. Similar results are observed in both the MeEug and Eug systems, where the Tg decreases to -0.67 °C and -1.4 °C for 50 mol % loadings, respectively (Figures S12 and S14). The systematic decrease in Tg can be attributed to the increasing incorporation of

monofunctional monomer and a decrease in crosslink density. The catechol moiety does not provide significant inter-network hydrogen bonding, and its incorporation diminishes the number of chemical crosslinks within the network structure and, hence, decreases the Tg. The EugOH systems show the lowest Tg values at all loading percentages because the catechol moiety is also limiting overall

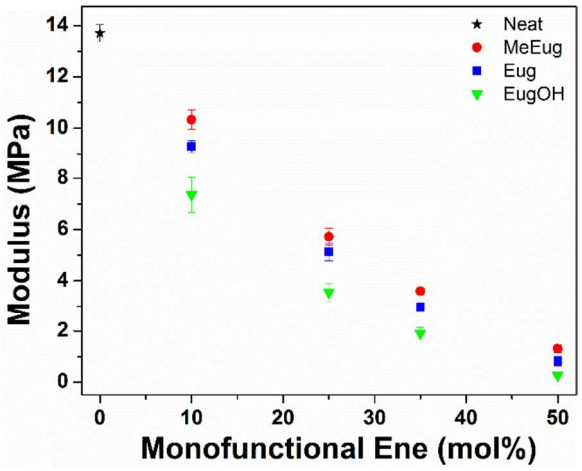

Fig. 7 Modulus as a function of monofunctional monomer content: MeEug (●), Eug (■), and EugOH (▼).

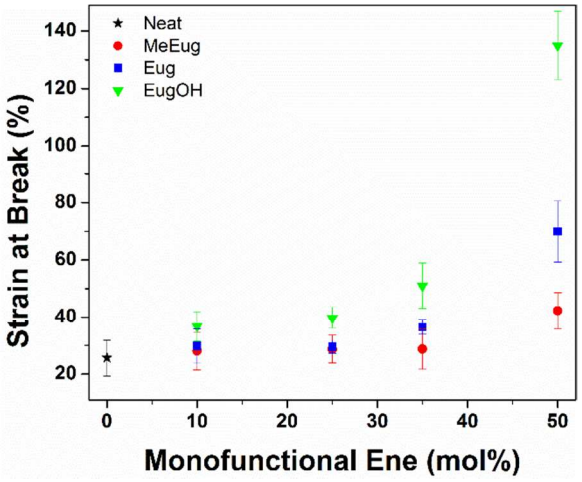

Fig. 8 Strain at break as a function of monofunctional monomer content: MeEug (●), Eug (■), and EugOH (▼).

monomer conversion, which contributes further to a decrease in chemical crosslinks. The effect of decreased conversion is exemplified in the 50 mol % EugOH-APE-PETMP network, where less complete and less uniform network formation causes a broadening in tan delta peak. These results contrast with our previous work, where we incorporated an amide containing monofunctional catechol monomer into an APE-PETMP network leading to an increase in Tg.[32] The amide provides significant hydrogen bonding sites within the network which act as physical crosslinks and serve to diminish the effect of increasing monofunctional monomer content and decreasing conversion. The lack of an amide in the EugOH systems results in thermomechanical properties being primarily dictated by decreases in crosslink density and conversion.

Young's modulus and elongation at break of the MeEug, Eug, and EugOH containing APE-PETMP networks were studied using tensile tests, and structure-property relationships of the networks were developed as a function of monofunctional monomer loading. Samples were prepared as previously described and cured into dog bones using UV irradiation. The

Table 3 Cross-hatch adhesion results for methyl eugenol, eugenol, and 4-allylpyrocatechol ternary polymer networks based on APE-PETMP on various substrates.

Thiol-Ene System	Aluminum	Glass	Steel	Marble
MeEug-APE-PETMP				
10:90	0B	0B	0B	0B
25:75	0B	0B	1B	1B
35:65	0B	0B	1B	3B
50:50	1B	1B	3B	3B
Eug-APE-PETMP				
10:90	0B	0B	0B	0B
25:75	0B	0B	2B	2B
35:65	0B	0B	3B	3B
50:50	2B	1B	4B	4B
EugOH-APE-PETMP				
10:90	0B	2B	1B	0B
25:75	1B	3B	2B	1B
35:65	4B	3B	4B	4B
50:50	5B	5B	5B	5B

samples were subjected to a strain rate 0.2 in/min and the Young's modulus and strain at break values are shown in Figures 7 and 8, respectively (numerical values provided in Table 2). The neat APE-PETMP system has the highest Young's modulus (13.7 ± 0.33 MPa), and the lowest strain at break (25.6 ± 6.27 %). Upon increasing monofunctional monomer concentration, the modulus begins to decrease and the strain at break gradually increases (until 50 mol %). Both the decrease in modulus and strain at break are attributed to the decrease in crosslink density with increasing monofunctional monomer content. The incorporation of the monofunctional alkene monomers introduces more free chain ends into the network, decreasing rigidity and therefore modulus, while enabling increased chain rearrangement upon network deformation. For example, the modulus values for the EugOH system decrease from 7.36 ± 0.68 MPa at 10 mol % loading to 0.266 ± 0.039 MPa at 50 mol % loading, while the strain at break values increase from 36.7 ± 5.27 % at 10 mol % loading to 135.0 ± 11.8 % at 50 mol % loading. Interestingly, the modulus decreases with increasing hydroxyl content in the monofunctional monomers, while the strain at break simultaneously increases. MeEug showed the highest modulus values, but lowest strains at break and contains no phenolic hydroxyl groups, while EugOH showed the lowest modulus values, and the largest strains at break, containing the dihydroxyl, catechol moiety (Eug shows intermediate values in

both cases). While it may be expected that the increase in hydroxyl content (MeEug to Eug to EugOH) would lead to increased hydrogen bonding within the network and therefore higher modulus values, similar to results observed in our thermomechanical testing, the phenolic and catechol hydroxyl groups lead to radical inhibition that outweighs any potential benefits from hydrogen bonding by lowering the overall polymerization conversion values. The decreases in conversion contribute further to a lowering of the crosslink density and therefore decreases in modulus and increases in strain at break. EugOH shows the lowest conversion values and crosslink densities thus, while inter-network hydrogen bonding may be present, the modulus of the ternary thiol-ene systems is dominated by the change in crosslink density.

Adhesive Properties

Adhesive behavior is a function of various factors, including chemistry, viscoelastic response, surface preparation, and substrate type. In this study, we wanted to investigate the effect catechol concentration had on the adhesive performance of the thiol-ene films. Using MeEug and Eug as controls should help to deconvolute, to some extent, the adhesive behavior resulting from changes in viscoelastic properties and the adhesive behavior resulting from changes in catechol monomer concentration. As previously described, MeEug, Eug, and EugOH ternary thiol-ene films were drawn down at 2 mils (~50 μm) onto aluminum, steel, glass, and marble substrates, cured, and subjected to the cross-hatch adhesion test.

The results from the cross-hatch adhesion test are summarized in Table 3. The neat system, as well as 10 mol % loadings of both the control, MeEug, and phenol containing monomer, Eug, showed similar results, with all films being classified as 0B on all substrate types. The films in each case were completely removed from the substrates as a result of the adhesion test. Both MeEug and Eug demonstrate increasing adhesion to steel and marble from 25 to 50 mol % loading, with Eug showing a higher rating for adhesion, having films classified at 2B at 25 mol % to 4B at 50 mol%. Because the MeEug system has no adhesive moiety, the increase in adhesion can be attributed to the change in viscoelastic properties. As the mol % of MeEug increases, the T_g decreases, leading to a tackier resin capable of more mechanical interlocking on the rough steel surface and porous marble surface. These viscoelastic changes do not lead to measureable increases in adhesion on glass or aluminium (until 50 mol %) because they are much smoother surfaces, and lack significant sites to facilitate mechanical adhesion. This same effect is observed in the Eug system, as the T_g decreases with increasing loading percentage, the adhesion values increase on steel and marble, but not aluminium or glass (until 50 mol %). The adhesion values for Eug, however, are greater when compared to the MeEug system due to the presence of the single hydroxyl moiety of Eug, capable of hydrogen bonding interactions with the substrate surface. While viscoelastic properties likely contribute to the increase in adhesion for the Eug system, the magnitude of change in the T_g values between MeEug and Eug at the various loading percentages are likely not significant enough to cause observable changes in adhesion.

The EugOH-APE-PETMP system, containing the known adhesive catechol moiety, shows significant increases in adhesion. The EugOH films show enhanced adhesion on all substrates at all loading percentages, compared to MeEug and Eug. Knowing the glass substrate is smooth compared to the other substrates, and strong adhesion was not observed for the MeEug and Eug systems, the increase in adhesion may be attributed to chemical interaction between the glass surface and

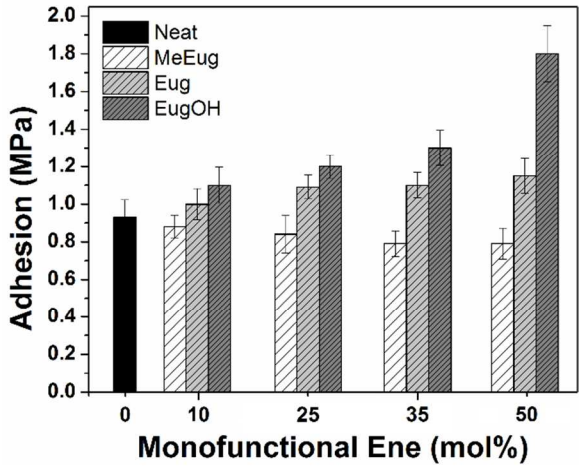

Fig. 9 *Lap shear adhesion values for MeEug, Eug, and EugOH ternary polymer networks on glass substrates.*

the catechol moiety. The EugOH films on glass are classified from 2B at 10 mol % to 5B at 50 mol %, significantly higher than the MeEug and Eug analogues. Similar results were observed on the other substrates as well, with adhesion values reaching 4B at 35 mol % and 5B at 50 mol % on aluminium, steel, and marble. Only light flaking was observed for films at 4B, while the 5B films remain perfectly intact, showing strong adhesion performance.

Additionally, lap shear adhesion testing was performed to develop a more thorough understanding of our thiol-ene adhesives. Due to our use of UV photopolymerization, only glass substrates were able to be prepared for lap shear testing. However, lap shear adhesion testing combined with cross-hatch adhesion testing, helps to elucidate and understand both the interfacial adhesive interactions, and the bulk cohesive interactions at work within our thiol-ene thin films. As shown in Figure 9, the EugOH system out-performs the MeEug and Eug systems at all mol % of monofunctional monomer loading, reaching an adhesion value of 1.8 ± 0.15 MPa at 50 mol % EugOH; significantly higher than the neat APE-PETMP system (0.93 ± 0.090 MPa). The Eug system shows slightly increased adhesion values from the neat system, but plateaus at approximately 1.1 MPa. The MeEug system however, shows the opposite trend; as the concentration of MeEug in the system is increased, a decrease in adhesion is observed. At first, this appears contradictory to our cross-hatch results. However, lap

shear adhesion also probes bulk cohesive interactions, which change as we incorporate more of the monofunctional alkene (i.e. the crosslink density is decreasing). Because MeEug has no significant chemical interaction with the substrate interface, and its crosslink density and modulus are being systematically decreased with increasing monofunctional monomer concentration, lower adhesion values are observed at higher mol % incorporation. The bulk material is becoming weaker, and with no increase in interfacial interaction like that observed for the Eug system, and more prominently, the EugOH system, the MeEug thiol-ene adhesive fails at lower forces.

Conclusions

We have reported the synthesis of catechol-functionalized thiol-ene polymer networks as photocurable adhesives, where the adhesive interactions are derived from 4-allylpyrocatechol – a monofunctional alkene readily obtained from natural products of *Syzygium aromaticum* flower buds (clove). The thiol-ene photopolymerization process enables rapid cure times, low energy input, and solvent-free processing. Increasing the concentration of EugOH in the thiol-ene networks resulted in improved adhesion on a variety of substrates, including glass, aluminium, steel, and marble. In addition, EugOH networks were studied in comparison to networks containing eugenol and methyl eugenol. These comparative studies illuminate the role catechol plays in dictating polymerization kinetics, mechanical, and thermomechanical properties, and adhesion in these thiol-ene materials. While adhesive properties have been imparted to the model APE-PETMP thiol-ene resin by incorporating a natural product catechol containing monomer, this same synthetic technique could be applied to variety of network materials leading to the generation of photocurable sealants, hydrogels, and adhesives for dental, biomedical, and advanced applications based on sustainable chemistries.

Acknowledgements

The authors gratefully acknowledge financial support from the National Science Foundation (NSF DMR-1041853 and NSF CAREER DMR-1056817). BRD thanks the US Dept. of Education GAANN Fellowship Program (Award # P200A120118) for financial support.

Notes and references

[a]*School of Polymers and High Performance Materials, The University of Southern Mississippi, 118 College Drive #5050, Hattiesburg, Mississippi 39406, United States*
[*]*Corresponding Author, E-mail:* Derek.Patton@usm.edu

Electronic Supplementary Information (ESI) available: [^{1}H and ^{13}C NMR, IR spectroscopy, thermomechanical and mechanical properties of MeEug and Eug networks]. See DOI: 10.1039/b000000x/

1. A. J. Kinloch, *J Mater Sci*, 1980, **15**, 2141-2166.
2. H. Zhao and J. H. Waite, *J. Biol. Chem.*, 2006, **281**, 26150-26158.
3. J. H. Waite and M. L. Tanzer, *Science*, 1981, **212**, 1038-1040.
4. P. B. Lee, P. B. Messersmith, J. N. Israelachvili and J. H. Waite, *Annu. Rev. Mater. Res.*, 2011, **41**, 99-132.
5. T. Lana-Villarreal, A. Rodes, J. M. Pérez and R. Gómez, *J. Am. Chem. Soc.*, 2005, **127**, 12601-12611.
6. S. A. Mian, X. Gao, S. Nagase and J. Jang, *Theor Chem Acc*, 2011, **130**, 333-339.
7. A. Akemi Ooka and R. L. Garrell, *Biopolymers*, 2000, **57**, 92-102.
8. J. Wang, M. N. Tahir, M. Kappl, W. Tremel, N. Metz, M. Barz, P. Theato and H. Butt, *Adv. Mater.*, 2008, **20**, 3872-3876.
9. J. Monahan and J. J. Wilker, *Langmuir*, 2004, **20**, 3724-3729.
10. P. A. Suci and G. G. Geesey, *J. Colloid. Inter. Sci.*, 2000, **230**, 340-348.
11. C. Fant, K. Sott, H. Elwing and F. Hook, *Biofouling*, 2000, **16**, 119-132.
12. L. A. Burzio and J. H. Waite, *Biochemistry*, 2000, **39**, 11147-11153.
13. L. M. Hight and J. J. Wilker, *J Mater Sci*, 2007, **42**, 8934-8942.
14. J. Heo, T. Kang, S. G. Jang, D. S. Hwang, J. M. Spruell, K. L. Killops, J. H. Waite and C. J. Hawker, *J. Am. Chem. Soc.*, 2012, **134**, 20139-20145.
15. R. Vendamme, N. Schüwer and W. Eevers, *J. Appl. Polym. Sci.*, 2014, **131**, DOI: 10.1002/app.40669.
16. M. Yu and T. J. Deming, *Macromolecules*, 1998, **31**, 4739-4745.
17. H. Tatehata, A. Mochizuki, T. Kawashima, S. Yamashita and H. Yamamoto, *J. Appl. Polym. Sci.*, 2000, **76**, 929-937.
18. M. Yu, J. Hwang and T. J. Deming, *J. Am. Chem. Soc.*, 1999, **121**, 5825-5826.
19. C. R. Matos-Pérez, J. D. White and J. J. Wilker, *J. Am. Chem. Soc.*, 2012, **134**, 9498-9505.
20. A. Stepuk, J. G. Halter, A. Schaetz, R. N. Grass and W. J. Stark, *Chem. Commun.*, 2012, **48**, 6238-6240.
21. W. Ma, H. Xu and A. Takahara, *Adv. Mater. Inter.*, 2014, **1**, DOI: 10.1002/admi.201300092.
22. H. J. Meredith, C. L. Jenkins and J. J. Wilker, *Adv. Func. Mater.*, 2014, **24**, 3259-3267.
23. E. M. White, J. E. Seppala, P. M. Rushworth, B. W. Ritchie, S. Sharma and J. Locklin, *Macromolecules*, 2013, **46**, 8882-8887.
24. H. Chung, P. Glass, J. M. Pothen, M. Sitti and N. R. Washburn, *Biomacromolecules*, 2010, **12**, 342-347.
25. J. Xue, T. Wang, J. Nie and D. Yang, *J. Appl. Polym. Sci.*, 2013, **127**, 5051-5058.
26. J. Xue, T. Wang, J. Nie and D. Yang, *J. Photoch. Photobio. B*, 2013, **119**, 31-36.
27. R. Schwalm, *UV Coatings: Basic, Recent Developments and New Applications*, Elsevier: Amsterdam, London, 2007.
28. C. E. Hoyle and C. N. Bowman, *Angew. Chem. Int. Ed.*, 2010, **49**, 1540-1573.
29. C. E. Hoyle, T. Y. Lee and T. J. Roper, *J. Polym. Sci. A: Polym. Chem.*, 2004, **42**, 5301-5338.
30. C. E. Hoyle, A. B. Lowe and C. N. Bowman, *Chem. Soc. Rev.*, 2010, **39**, 1355-1387.
31. A. B. Lowe, *Polym. Chem.*, 2014, DOI: 10.1039/C1034PY00339J.
32. B. J. Sparks, E. F. T. Hoff, L. P. Hayes and D. L. Patton, *Chem. Mater.*, 2012, **24**, 3633-3642.
33. H. Bilel, N. Hamdi, F. Zagrouba, C. Fischmeister and C. Bruneau, *RSC Advances*, 2012, **2**, 9584-9589.
34. G. P. Kamatou, I. Vermaak and A. M. Viljoen, *Molecules*, 2012, **17**, 6953-6981.
35. , ASTM International, West Conshohocken, PA, 2009.
36. , ASTM Internationl, West Conshohocken, PA, 2010.
37. J. M. Blackwell, K. L. Foster, V. H. Beck and W. E. Piers, *J. Org. Chem.*, 1999, **64**, 4887-4892.
38. W. H. Daly and S. J. Moulay, *J. Polym. Sci.: Polym. Symp.*, 1986, **74**, 227-242
39. Y. Ai, J. Nie, G. Wu and D. Yang, *J. Appl. Polym. Sci.*, 2014, DOI: 10.1002/app.41102.
40. P. J. Flory, *Polymer*, 1979, **20**, 1317-1320.
41. Q. Li, H. Zhou and C. E. Hoyle, *Polymer*, 2009, **50**, 2237-2245.

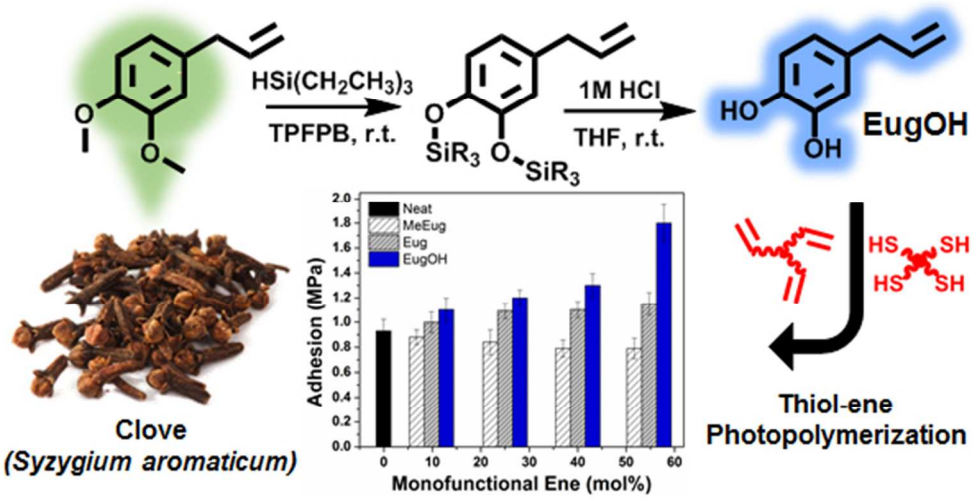

161x82mm (96 x 96 DPI)